THE SOURCE OF THE DISPERSITY OF GRAMICIDIN A SINGLE-CHANNEL CONDUCTANCES

The L · Leu[5]-Gramicidin A Analog

D. W. URRY, S. ALONSO-ROMANOWSKI, C. M. VENKATACHALAM, T. L. TRAPANE, AND K. U. PRASAD

Laboratory of Molecular Biophysics, University of Alabama in Birmingham, School of Medicine, Birmingham, Alabama 35294

ABSTRACT The L · Leu[5]-gramicidin A analog has been designed, synthesized, and verified for the purpose of testing the perspective that different side-chain distributions are responsible for the dispersity of single-channel conductances. The structural analysis shows that the L · Leu[5] analog would limit the possible number of side-chain distributions and that the dispersity of channel conductances would decrease. The finding is the expected decrease in less probable conductance states and the associated increase in the probability of the most probable conductance state.

INTRODUCTION

A histogram containing the frequency of occurrence of gramicidin A (HCO—L · Val[1]—Gly[2]—L · Ala[3]—D—Leu[4]—L · Ala[5]—D · Val[6]—L · Val[7]—D · Val[8]—L · Trp[9]—D · Leu[10]—L · Trp[11]—D · Leu[12]—L · Trp[13]—D · Leu[14]—L · Trp[15]—$NHCH_2CH_2OH$) single-channel conductances in planar lipid bilayer membranes demonstrates a most probable distribution of conductances and also exhibits a broad range of less probable, lesser conducting states. This is seen in Fig. 1 where, at 20°C, ~60% of the events occur in distribution centered on 17 ± 1.5 pS, whereas the remaining 40% of the events are spread primarily over the range from 6 to 15 pS. To achieve an adequate understanding of gramicidin A (GA) channel transport, it is essential to determine the source of this dispersity of single-channel conductances. In appreciating the significance of the planar lipid bilayer studies, it is important to realize that single channels are being observed and that a single channel turns on at a given conductance and generally maintains that conductance over the lifetime of the channel. In the initial studies (1) this dispersity could have been due in part to the mix of analogs in the natural preparation but, more recently, a high performance liquid chromatography (HPLC) purified natural GA and a wholly synthetic GA gave similar histograms with equivalent dispersity as in Fig. 1 (2). Dispersity had similarly been reported for synthetic gramicidin C (i.e., Tyr[11]—GA) (3). Another source of the multiplicity of single-channel conductances could be a mix

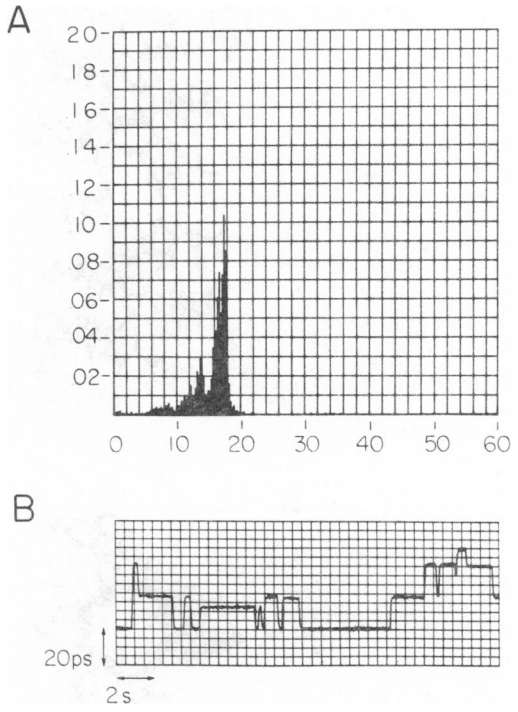

FIGURE 1 Histograms of the frequency of occurrence of single-channel conductances (*A*) and single-channel conductance trace (*B*) of HPLC purified synthetic (1-[13]C)L · Val[1]-GA (13) in diphytanoyl/*n*-decane membranes at 20°C, 100 mV, and 1 M KCl. About 60% of the channel events occur in the most probable conductance peak defined as the 17 ± 1.5 pS window. Sample purification and handling and planar bilayer conditions are identical to that for L · Leu[5]-GA in Fig. 6. In *A* n = 1,513 and ⟨cond⟩, the mean value of, is 15.56 pS at 20.1°C.

of channel conformations (e.g., single- and double-stranded β-helices with different numbers of residues per turn and with different end-to-end associations), but the studies designed to delineate structure strongly argue that more than 90% of the channels are head-to-head dimerized single-stranded β-helices, both in planar bilayers (4, 5) and in suspensions of bilayer membranes (6, 7). Accordingly, different channel radii, hydrogen bonding defects or variants, and distributions of side-chain orientations have now been suggested (8–10). The L · Leu^5-GA analog was synthesized to test the perspective of different side-chain distributions resulting in different distributions of single-channel conductances. The arguments begin with a careful analysis of molecular structure.

A side view of the calculated in vacuo molecular structure of the dimeric GA channel is given in stereo in Fig. 2 *A* and the channel view from solution of one monomer is given in Fig. 2 *B*. This is the in vacuo most preferred conformation of a family of competing conformational states involving differences primarily in side-chain orientations. The presence of the bulky side chains restricts the possible orientations of adjacent side chains along the sequence and between turns of the helix (9, 10). This involves steric interactions between the side chains of residue i and those of residues i ± 1 and i ± 6. Because interchange between some energetically similar distributions of side chains requires simultaneous, concerted movement of several side chains, it has been proposed that the interconversion can be slow giving lifetimes for changing conductance state on the order of seconds (9, 10).

Of particular interest in Fig. 2 is a comparison of the orientations of the Trp^9 and Trp^{15} side chains with the orientation of the Trp^{11} side chain. The small Ala^3 side chain allows Trp^9 (and consequently Trp^{15}) to be oriented toward the formyl end of the molecule with the Trp^9 indole ring lying over the methyl moiety of residue 3. The Trp^{11} side chain is seen with an opposite orientation, i.e., directed outward toward the solution similar to that of Trp^{13}. Because residue 5 is an Ala, however, the Trp^{11} side chain could also be oriented over the methyl moiety of residue 5 just as the Trp^9 side chain is over residue 3. The Trp^{13} side chain, on the other hand, does not orient like that of Trp^9 in part due to the bulkier side chain of Val^7. A bulkier side chain in position 5 should serve to prevent the Trp^9-like orientation of the Trp^{11} side chain. Our working hypothesis is that changes in critical side chain orientations, by

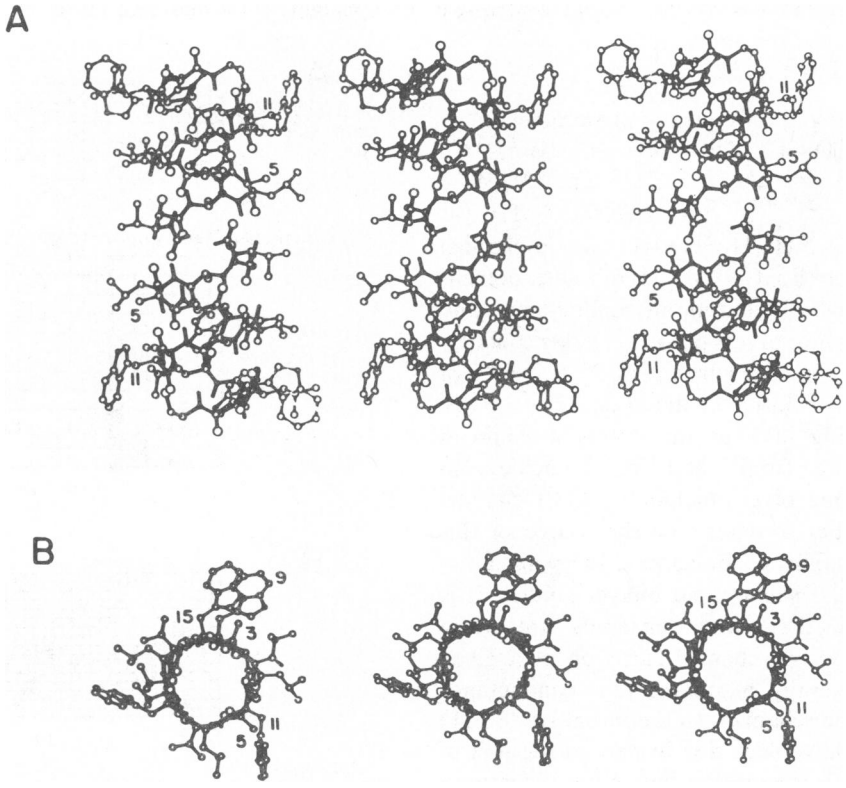

FIGURE 2 Stereo pair plots of the in vacuo most favorable conformation of the gramicidin A transmembrane channel. (*A*) side view (*B*) channel view of monomer from solution. This is one of a set of energetically comparable conformations that differ in terms of the side-chain orientations. This structure, then, represents one of the side-chain distributions. To facilitate viewing, the stereo pairs are arranged for either close (cross-eye) or distance (wall-eye) viewing. For cross-eye viewing, place a piece of paper over the right-hand structure leaving the left-hand pair. For wall-eye viewing, cover the left-hand structure. Note in particular the orientation of the Trp side chains. In the side view, it is seen that the Trp^{11} indole could rotate to lay over the Ala^5 methyl as does the Trp^9 indole over the Ala^3 methyl (seen in channel view). Changing this orientation of the Trp^{11} side chain is expected to change the energy of the barrier for ion entry into the channel by changing the energy of the peptide moiety libration required to achieve ion coordination. Reproduced with permission from reference 10.

altering the energetics of the involved residues' peptide librations required for ion coordination, could give rise to a different single-channel current and would, thereby, be responsible for the dispersity of single-channel currents. Specifically in the histogram of the frequency of occurrence of single-channel conductances of GA in diphytanoyl lecithin/*n*-decane membranes at 1 M KCl, 100 mV, and 20°C in Fig. 1, the less probable, lower conducting states would result from less frequently occurring side-chain distributions. A direct test of this hypothesis is to synthesize and characterize the L · Leu[5] analog of GA. This is expected to prevent the side chain of Trp[11] from assuming an orientation (perhaps a slightly less probable state) like that of Trp[9] and cause it to orient as seen for Trp[13]. The expected result is that the multiplicity of single-channel conductances obtained under identical experimental and analytical conditions will decrease and there will be a greater frequency of occurrence for the most probable state.

MATERIALS AND METHODS

Synthesis

The synthesis of L · Leu[5]-GA was carried out by the method of solid-phase peptide synthesis (11) with a few modifications as described earlier from this laboratory (2, 12, 13). In the present synthesis, the β-indole ring of the Trp residues was protected by a formyl group (14, 15) to prevent air oxidation under acidic conditions. After the synthesis was completed, the *N*-protected peptide was removed from the resin by ethanolamine treatment and under these conditions the N^{indole}-formyl group on tryptophyl residue was also removed. After deblocking the NH_2-terminal protecting group, the desformyl gramicidin analog was formylated and purified by preparative thin layer chromatography followed by LH-20 column chromatography (Pharmacia Fine Chemicals, Piscataway NJ). The purity of the product was checked by proton and carbon-13 nuclear magnetic resonance (NMR) spectroscopy and by HPLC as described below.

Characterization by NMR

Carbon-13 NMR spectra of commercially available natural GA and of the synthetic L · Leu[5]-GA in dimethyl-D_6-sulphoxide were obtained on a spectrometer (PFT-100; JEOL USA, Analytical Instruments Div., Cranford, NJ) operating at 25 MHz and 30°C. The spectra are given in Fig. 3 where assignments are included for the natural gramicidin mixture (2, 16). Note the absence of any detectable impurities in the synthetic L · Leu[5]-GA as well as the loss of an alanine α-carbon resonance along with the addition of a leucine α-carbon. Proton NMR spectra in dimethyl-D_6-sulphoxide of these gramicidins were also obtained utilizing a spectrometer (HR-220; Varian Associates, Inc., Palo Alto, CA) operating at 220 MHz and 20°C. Spectral assignments in Fig. 4 are given for the natural GA (17). The purity of the synthetic L · Leu[5] analog is readily seen as well as the loss of the alanine β-methyl protons and the addition of leucine β-methylene and δ-methyl resonances. These spectra verify the correctness and purity of the L · Leu[5]-GA analog.

HPLC Purification for Bilayer Studies

The absence of extraneous peaks and the presence of the specific changes required in the NMR spectra of L · Leu[5]-GA in comparison with those of GA demonstrates the material to be greater than 95% pure. Thus, when this material is passed through an analytical HPLC column, the major peak is clearly the desired analog. This peak is collected and repassed through the analytical HPLC column. After several passes, a fraction of the sample peak is collected for the planar bilayer studies. This assures that the analog is indeed the desired product and that it is obtained at the highest possible level of purity. This seeming obsession for purity is understood when it is appreciated that individual single-channel events are being observed and that certain impurities could give rise to apparent dispersity of single-channel currents. Comparison is to be made between histograms of synthetic GA of Fig. 1 and of L · Leu[5]-GA. Both have been treated identically and the dispersity observed in Fig. 1 is similar to that observed by others for pure GA using the same membranes (18). The HPLC chromatograms are given in Fig. 5.

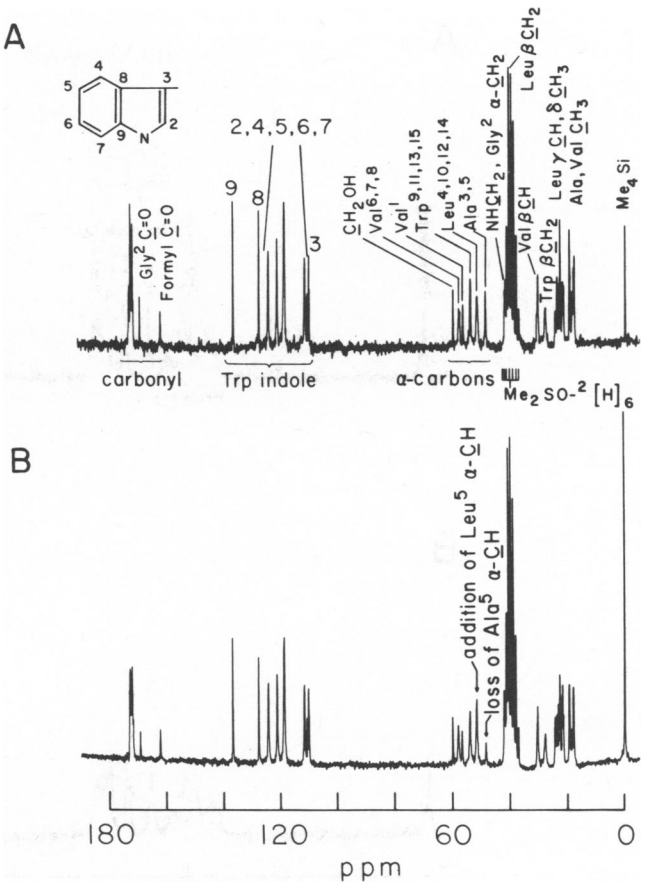

FIGURE 3 Carbon-13 magnetic resonance spectra at 25 MHz in dimethyl-D_6-sulphoxide at 30°C for (*A*) natural GA and (*B*) synthetic L · Leu[5]-GA.

Planar Bilayer Studies

Black lipid membranes were formed on a 0.6-mm diam aperture separating two Teflon chambers, each filled with 7 ml of 1 M KCl solution, as previously described (19, 20). The lipid solution used in forming the membrane was diphytanoyl lecithin (DPhL) 2% (wt/vol) in *n*-decane. Picomolar concentrations of HPLC purified L/eu[5]—GA were added to the bath from methanolic stock solutions. Samples were always added in comparable amounts using the same organic solvent. Data were acquired only after a certain period of time (~1 h). The temperature of the cell was maintained within ±0.1°C by means of a Peltier cell. Temperature of the cell was controlled by a power supply built in this laboratory (21) and two Peltier thermoelectric modules from MELCOR (Trenton, NJ). The membrane voltage clamp was 100 mV using a battery-operated voltage source through Ag-AgCl electrodes.

The membrane cell was contained in a metal box, mounted on a vibration free table (Micro-g; Technical Manufacturing Corporation, Woburn, MA). The signal from the cell membrane was delivered either to

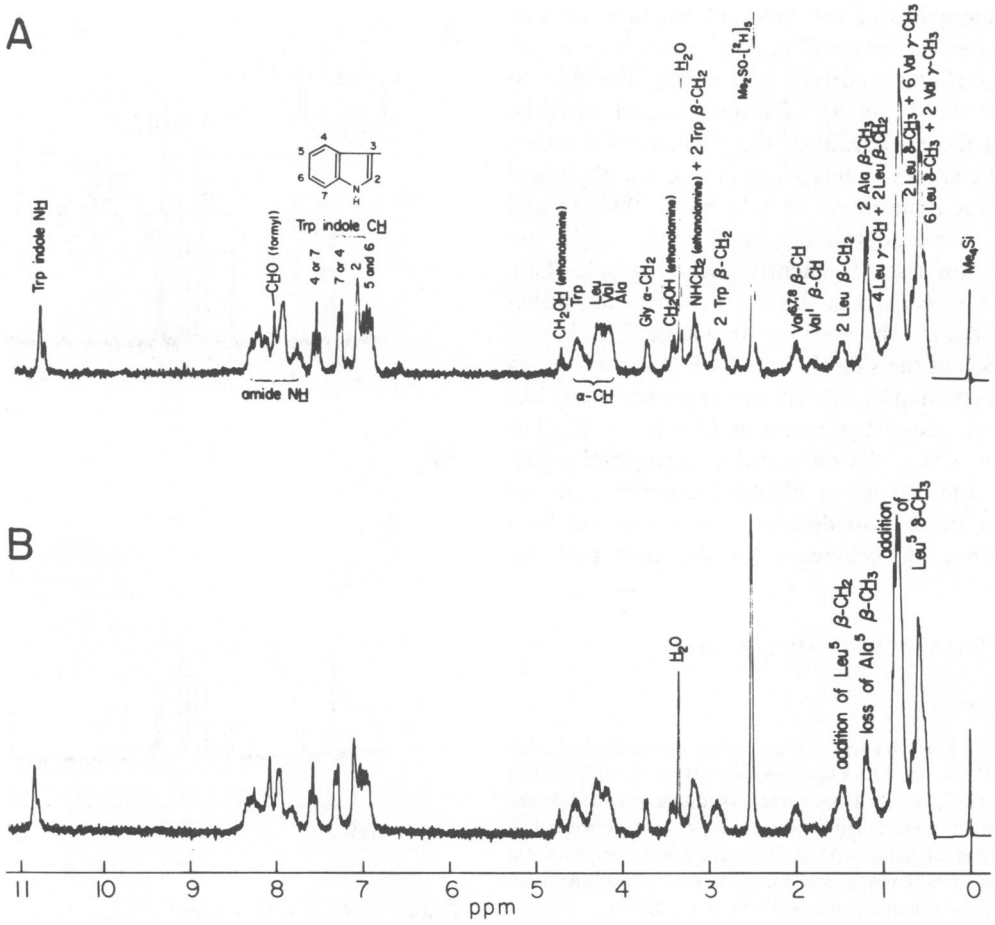

FIGURE 4 Proton magnetic resonance spectra at 220 MHz in dimethyl-D_6-sulphoxide at 20°C for (*A*) natural GA and (*B*) synthetic L · Leu^5-GA.

a current amplifier set (427; Keithley Instruments, Inc., Cleveland, OH) with a rise time of 0.03 ms or to a low noise, low drift, precision FET amplifier (model 52; Analog Devices, Inc., Norwood, MA). The output from the amplifier was passed through a filter (3342; Krohn-Hite Corp., Avon, MA) that was kept in the low pass resistance-capacitance mode in the range 50–100 Hz. The single-channel events were monitored and recorded in a storage oscilloscope (2090; Nicolet Instrument Corp., Madison, WI), where a maximum of 4,096 data points can be recorded in one sweep. Using a 5-ms sampling time per point, a single sweep spanned a time window of 20.48 s. The recorded sweeps were transferred from the storage oscilloscope to a computer (4054A; Tektronix, Inc., Beaverton, OR) through an RS-232 interface.

Analysis of Conductance Traces

Sweeps of single-channel conductance traces were analyzed in the computer (Tektronix, Inc.) equipped with signal processing read-only memory (ROM) packs. The conductance transition detection was realized by computing the time points where the derivative of the signal exceeded a suitably chosen threshold value, a procedure somewhat similar to the method employed recently by Andersen (18). Having thus determined all the transitions in a given sweep, the single-channel events occurring in the sweep were deduced by properly matching the downward transitions with their corresponding upward transitions, thereby obtaining an estimate of the dwell time (i.e., lifetime) of the channel event. The matching algorithm was based on comparing the heights of the downward and upward transitions and will be fully described elsewhere (21).

RESULTS AND DISCUSSION

In approaching the question of the distribution of single-channel conductances, it is important to be aware that the planar bilayer study of GA channel transport involves a system that is not at equilibrium. Thus, the history of the system before channels are observed becomes relevant. GA is usually added as an organic solution to both sides of the aqueous bath. As GA is insoluble in water, there would be aggregation occurring on addition to the bath that is in part dependent on the organic solvent state. The observation that *N*-Ac-L · Pro-desformyl-GA forms no more than a few percent of the channel conformation when heated with L-α-lysolecithin (Urry, D. W., S. Alonso-Romanowski, C. M. Venkatachalam, T. L. Trapane, and K. U. Prasad, unpublished results) suggests that monomers in the β-helical conformation are not diffusing around in the lipid until they happen on a monomer tied to the other side of the membrane, but rather that monomers form in the single-stranded β-helical conformation at the interface, transiently dip into the lipid layer and remain there only if a second monomer is appropriately encountered and a lipid spanning head-to-head dimeric channel results. There is

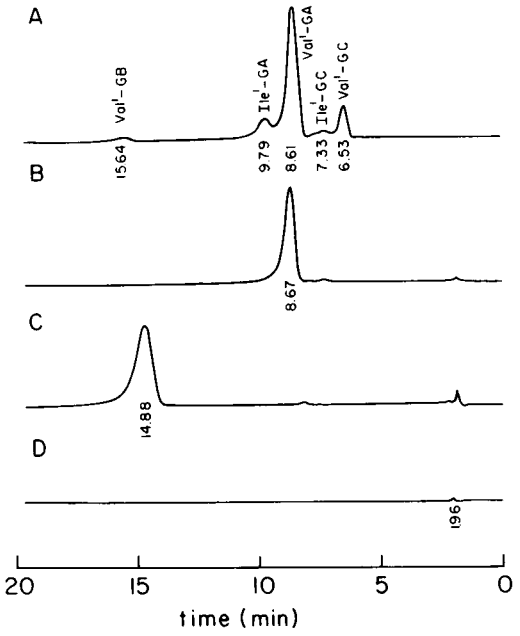

FIGURE 5 HPLC chromatograms of (*A*) natural gramicidin, which is a mixture of at least five analogs (GB = L · Phe[11]-GA and GC = L · Tyr[11]-GA), (*B*) synthetic (1-[13]C) Val[1]-GA, (*C*) L · Leu[5]-GA and (*D*) blank for solvent on Zorbax ODS analytical column with 15% water in methanol as solvent. These chromatograms demonstrate the high level of purity achieved in the syntheses. The corresponding carbon-13 and proton NMR spectra, which verify the correct structures, are shown in Figs. 3 and 4. For the transport studies, a peak is collected, passed several more times through the column and in the last pass a fraction of the peak is collected for use in the planar bilayer studies.

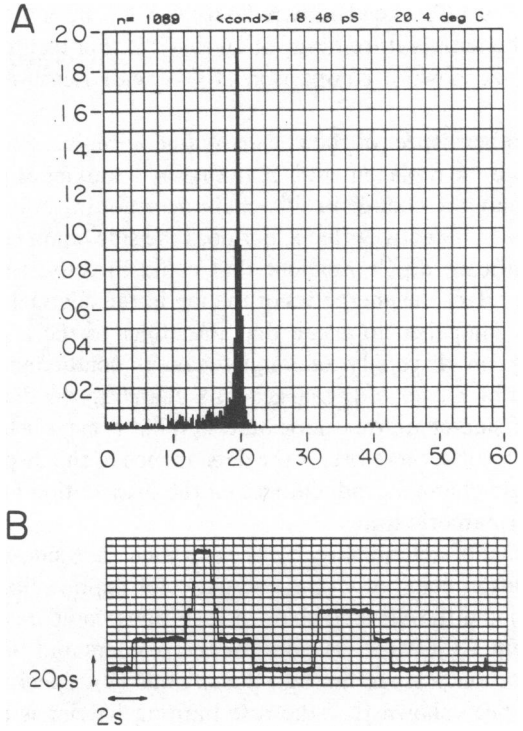

FIGURE 6 Histogram of the frequency of occurrence of single-channel conductances (*A*) and single-channel conductance trace (*B*) of HPLC purified L · Leu[5]-GA. The sample purification and handling and the planar bilayer measurement conditions are identical to those used for GA in Fig. 1. There is a striking increase in the probability of the most probable conductance states and a decrease in frequency of occurrence of the less probable, lesser conducting states. This demonstrates that altering side-chain distribution can alter the dispersity of single-channel conductance. In *A* n = 1,089 and ⟨cond⟩, the mean value of, is 18.46 pS at 20.4°C.

not expected to be an equilibrium distribution of side chains at the interface that would be relevant to an equilibrium distribution for the conducting state. Also the length of time that a channel exists is not sufficient to achieve an equilibrium distribution for the conducting state. A near equilibrium state could be approached with sufficient time once new aggregates have stopped appearing at the membrane aqueous interface. Our approach is to add the molecules in the same organic solvent at the same concentration and to compare data from membrane after a comparable period of time, e.g., 1 h, has elapsed.

As discussed in the Introduction, L · Leu[5]-GA was designed and synthesized for the purpose of producing a channel with some limiting of side-chain distributions. The expectation for this analog is that if different side-chain distributions are responsible for the dispersity of single-channel conductances, then L · Leu[5]-GA should exhibit a decrease in this dispersity, i.e., there should be an increase in the fraction of events in the most probable conducting state. This was observed, as shown in Fig. 6 where the probability of single-channel conductances are plotted as a function of the magnitude of conductance step for L · Leu[5]-GA at 20°C, 100 mV, 1 M KCl, and in diphytanoyl lecithin/*n*-decane membranes. Compare Figs. 1 *B* and 6 *B* to see how faithfully the single-channel current trace reproduces the same step for L · Leu[5]-GA but shows some variation for GA. Also comparing the histograms of Figs. 1 and 6, it is apparent that GA exhibits more events of conductance lower than the most probable events than does L · Leu[5]-GA. For example, using the same conductance width centered on the most probable state, for GA 49% of the events occur in the 16.50 to 18.25 pS conductance window, whereas for L · Leu[5]-GA, 68% of the events occur in the 19.25 to 21.00 pS conductance window. As there are more than 1,000 channels observed, where the "off" transition has been matched to an "on" transition, the statistical significance of the results is reasonably established.

Histograms for Leu[5]—GA have been obtained five times at 20°C and using different experimental set ups, twice with the Keithley (Keithley Instruments, Inc.) and three times with the Analog Devices (Analog Devices, Inc.) amplifier. This involved five different membranes on five different days, totaling some tens of thousands of events for Leu[5]—GA alone. Also the result of the decreased dispersity of single-channel currents exhibited

by Leu[5]—GA when compared with GA has been observed over the temperature range of 16 to 47°C. For example, in Fig. 7 is shown a comparison of GA with Leu[5]—GA at 39°C.

Another aspect of the choice of analog requires stating. Because the replacement is a methyl by a bulkier aliphatic R group, the change in side chain does not introduce any change in inductive effects, nor does the side chain contain a significant dipole moment that could directly, through space, affect the energetics of the ion in the channel. Thus one is compelled to argue that the effect of the L · Leu[5] analog on dispersity of single-channel conductances is indeed by means of the larger bulk changing the distribution of side-chain rotameric states. What is established by these results, therefore, is the dependence of the dispersity of single-channel conductances on the distribution of side-chain rotameric states.

It has, of course, already been argued that side-chain orientation could alter the energetics of peptide libration and that different side-chain orientations could result in different Gibbs free energies for the barriers and binding sites for ion passage through the channel (9). Specifically, it has been shown that the rate-limiting barrier is at the mouth of the channel (22–24) and that the carbonyls of Trp residues 9, 11, 13, and 15 dominate the ion binding sites (25). Accordingly, changes in the possible orientations of the Trp side chains and most directly of the side chains of residues 11, 13, and 15 would be expected to result in changes in the dispersity of single-channel conductances. In particular, molecular mechanics calculations in vacuo have shown four dominant rotameric states for the Trp[11] side chain of GA only two of which remain after Leu[5] substitution and the energies of these two states differ by 1.8 kcal/mol (26). The effect of L · Leu[5] replacement of L · Ala[5] is to restrict the possible L · Trp[11] side-chain orientations (as suggested by Fig. 2 and the discussion in the Introduction) and the result of L · Leu[5]-GA having a decrease in dispersity of channel states is to be expected when the source of dispersity is side-chain distributions.

Finally note that in the distribution of the most probable conductance state of GA (see Fig. 1) and perhaps even in the narrower distribution for L · Leu[5]-GA (see Fig. 6) there is a finite width beyond what may be considered to be the baseline noise. This means that there are different conductance substates within the most probable conductance state again with lifetimes of the order of seconds or longer. In our perspective, these would be due to smaller perturbations arising from side-chain orientation differences.

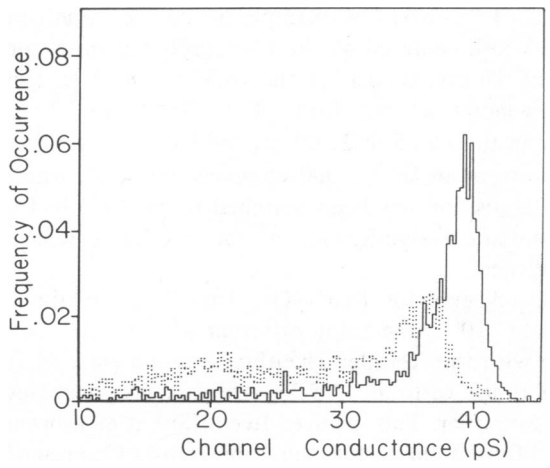

FIGURE 7 Histogram of the frequency of occurrence of single-channel conductances for GA at 39.7°C (· · ·) with 1,599 events and for L · Leu[5]-GA at 39.1°C (——) with 1,570 events.

This work was supported in part by the National Institutes of Health, Grant No. GM-26898.

Received for publication 13 December 1983 and in final form March 1984.

REFERENCES

1. Hladky, S. B., and D. A. Haydon. 1972. Ion transfer across lipid membranes in the processes of gramicidin A. I. Studies of the unit conductance channel. *Biochim. Biophys. Acta.* 274:294–312.
2. Prasad, K. U., T. L. Trapane, D. Busath, G. Szabo, and D. W. Urry. 1982. Synthesis and characterization of 1-^{13}C-D · Leu^{12,14} gramicidin A. *Int. J. Pept. Protein Res.* 19:162–171.
3. Bamberg, E., K. Noda, E. Gross, and P. Läuger. 1976. Single-channel parameters of gramicidin A, B and C. *Biochim. Biophys. Acta.* 419:223–228.
4. Apell, H.-J., E. Bamberg, H. Alpes, and P. Läuger. 1977. Formation of ion channels by a negatively charged analog of gramicidin A. *J. Membr. Biol.* 31:171–188.
5. Bamberg, E., H.-J. Apell, and H. Alpes. 1977. Structure of the gramicidin A channel: Discrimination between the $\pi_{L,D}$ and the β-helix by electrical measurements with lipid bilayer membranes. *Proc. Natl. Acad. Sci. USA.* 74:2402–2406.
6. Weinstein, S., B. A. Wallace, E. R. Blout, J. S. Morrow, and W. Veatch. 1979. Conformation of gramicidin A channel in phospholipid vesicles: A ^{13}C and ^{19}F nuclear magnetic resonance study. *Proc. Natl. Acad. Sci. USA.* 76:4230–4234.
7. Urry, D. W., T. L. Trapane, and K. U. Prasad. 1983. Is the gramicidin A transmembrane channel single-stranded or double-stranded helix? A simple unequivocal determination. *Science (Wash. DC).* 221:1064–1067.
8. Busath, D., and G. Szabo, 1981. Gramicidin forms multi-state rectifying channels. *Nature (Lond.).* 294:371–373.
9. Urry, D. W., C. M. Venkatachalam, K. U. Prasad, R. J. Bradley, G. Parenti-Castelli, and G. Lenaz. 1981. Conduction processes of the gramicidin channel. *Int. J. Quantum Chem. Symp.* 385–399.
10. Venkatachalam, C. M., and D. W. Urry. 1983. Theoretical conformational analysis of the gramicidin A transmembrane channel. Part I. Helix sense and energetics of head-to-head dimerization. *J. Computational Chemistry.* 4:461–469.
11. Merrifield, R. B. 1963. Solid phase peptide synthesis. I. The synthesis of a tetrapeptide. *J. Am. Chem. Soc.* 85:2149–2154.
12. Prasad, K. U., T. L. Trapane, D. Busath, G. Szabo, and D. W. Urry. 1983. Synthesis and characterization of (1-^{13}C) Phe^{9} gramicidin A. Effects of side chain variations. *Int. J. Pept. Protein Res.* 22:341–347.
13. Urry, D. W., T. L. Trapane, S. Romanowski, R. J. Bradley, and K. U. Prasad. 1983. Use of synthetic gramicidins in the determination of channel structure and mechanism. *Int. J. Pept. Protein Res.* 21:16–23.
14. Ohno, M., S. Tsukamoto, and N. Izumiya. 1972. Solid-phase synthesis of tryptophan-containing peptides. *J. Chem. Soc.* 663–664.

15. Ohno, M., S. Tsukamoto, S. Makisumi, and N. Izumiya. 1972. Improved solid-phase synthesis of tryptophan containing peptides. I. Use of hydrogen chloride in formic acid as a reagent for the cleavage of t-butyloxy carbonyl group. *Bull. Chem. Soc. Jpn.* 45:2852–2855.
16. Fossel, E. T., W. R. Veatch, Y. A. Ovchinnikov, and E. R. Blout. 1974. A ^{13}C nuclear magnetic resonance study of gramicidin A in monomer and dimer forms. *Biochemistry.* 13:5264–5275.
17. Glickson, J. D., D. F. Mayers, J. M. Settine, and D. W. Urry. 1972. Spectroscopic studies on the conformation of gramicidin A'. Proton magnetic resonance assignments, coupling constants, and H-D exchange. *Biochemistry.* 11:477–486.
18. Andersen, O. S. 1983. Ion movement through gramicidin A channels. Single-channel measurements at very high potentials. *Biophys. J.* 41:119–133.
19. Bradley, R. J., W. O. Romine, M. M. Long, T. Ohnishi, M. A. Jacobs, and D. W. Urry. 1977. Synthetic peptide K^+ carrier with Ca^{2+} inhibition. *Arch. Biochem. Biophys.* 178:468–474.
20. Bradley, R. J., D. W. Urry, K. Okamoto, and R. S. Rapaka. 1978. Channel structures of gramicidin. Characterization of succinyl derivatives. *Science (Wash. DC).* 200:435–437.
21. Urry, D. W., S. Alonso-Romanowski, C. M. Venkatchalam, and R. J. Bradley. 1984. Temperature dependence of single channel currents and the peptide libration mechanism for ion transport through the gramicidin A transmembrane channel. *J. Membr. Biol.* In press.
22. Urry, D. W., C. M. Venkatachalam, A. Spisni, P. Läuger, and M. A. Khaled. 1980. Rate theory calculation of gramicidin single-channel currents using NMR-derived rate constants. *Proc. Natl. Acad. Sci. USA.* 77:2028–2032.
23. Urry, D. W., C. M. Venkatachalam, A. Spisni, R. J. Bradley, T. L. Trapane, and K. U. Prasad. 1980. The malonyl gramicidin channel: NMR-derived rate constants and comparison of calculated and experimental single-channel currents. *J. Membr. Biol.* 55:29–51.
24. Finkelstein, A., and O. S. Andersen. 1981. The gramicidin A channel. A review of its permeability characteristics with special reference to the single-file aspect of transport. *J. Membr. Biol.* 59:155–171.
25. Urry, D. W., K. U. Prasad, and T. L. Trapane. 1982. Location of monovalent cation binding sites in the gramicidin channel. *Proc. Natl. Acad. Sci. USA.* 79:390–394.
26. Venkatachalam, C. M., S. Alonso-Romanowski, K. U. Prasad, and D. W. Urry. 1984. The Leu^5 gramicidin A analog: Molecular mechanics calculations and analysis of single channel steps related to multiplicity of conducting states. *Int. J. Quantum Chem. Symp. No. 11.* In press.